Analysis of the Cruciform Binding Activity of Recombinant 14-3-3ζ-MBP Fusion Protein, Its Heterodimerization Profile with Endogenous 14-3-3 Isoforms, and Effect on Mammalian DNA Replication in Vitro†

David Alvarez,‡,§ Mario Callejo,‡,§ Rami Shoucri,‡ Lee Boyer,§ Gerald B. Price,§ and Maria Zannis-Hadjopoulos*,‡,§

McGill University Department of Biochemistry and McGill Cancer Center Montreal, Canada H3G 1Y6

Received December 11, 2002; Revised Manuscript Received April 23, 2003

ABSTRACT: The human cruciform binding protein (CBP), a member of the 14-3-3 protein family, has been recently identified as an origin of DNA replication binding protein and involved in DNA replication. Here, pure recombinant 14-3-3ζ tagged with maltose binding protein (r14-3-3ζ-MBP) at its N-terminus was tested for binding to cruciform DNA either in the absence or presence of F_{TH}, a CBP-enriched fraction, by electromobility shift assay (EMSA), followed by Western blot analysis of the electroeluted CBP−cruciform DNA complex. The r14-3-3ζ-MBP was found to have cruciform binding activity only after preincubation with F_{TH}. Anti-MBP antibody immunoprecipitation of F_{TH} preincubated with r14-3-3ζ-MBP, followed by Western blot analysis with antibodies specific to the *β*, *γ*, *ϵ*, *ζ*, and *σ* 14-3-3 isoforms showed that r14-3-3ζ-MBP heterodimerized with the endogenous *β*, *ϵ*, and *ζ* isoforms present in the F_{TH} but not with the *γ* or *σ* isoforms. Immunoprecipitation of endogenous 14-3-3ζ from nuclear extracts (NE) of HeLa cells that were either serum-starved (s-s) or blocked at the G_1/S or G_2/M phases of the cell cycle revealed that at G_1/S and G_2/M, the *ζ* isoform heterodimerized only with the *β* and *ϵ* isoforms, while in s-s extracts, the 14-3-3ζ/*ϵ* heterodimer was never detected, and the 14-3-3ζ/*β* heterodimer was seldom detected. Furthermore, addition of r14-3-3ζ-MBP to HeLa cell extracts used in a mammalian in vitro replication system increased the replication level of p186, a plasmid bearing the minimal 186-bp origin of the monkey origin of DNA replication *ors*8, by approximately 3.5-fold. The data suggest that specific dimeric combinations of the 14-3-3 isoforms have CBP activity and that upregulation of this activity leads to an increase in DNA replication.

Origins of DNA replication contain inverted repeat sequences (IR),[1] which are associated with the initiation of DNA replication in mammals (*1*−*5*) and are able to extrude into a secondary DNA structure known as a cruciform in vivo (*6*) and in vitro (*7*−*9*). Several studies have provided evidence that cruciform DNA plays a role in the initiation of DNA replication (*4*, *10*−*13*), and a cruciform DNA binding protein (CBP) has been purified from HeLa cell extracts (*14*). Hydroxyl radical footprinting predicted a U-shaped structure for CBP (*15*), which was subsequently identified as a member of the 14-3-3 family of proteins (*16*), whose crystal structure (*17*) matched the one predicted by the footprinting. CBP/14-3-3 is involved in mammalian DNA replication and associates in vivo with the monkey origins of DNA replication *ors*8 and *ors*12 in a cell cycle-dependent manner, the association being higher at the G_1/S boundary (*18*−*20*). Furthermore, it was recently demonstrated that the yeast 14-3-3 homologues, Bmh1p and Bmh2p, also have cruciform binding activity and associate in vivo with the autonomous replication sequence (ARS) 307 (*21*).

The 14-3-3 family of proteins is expressed in all eukaryotic cells and is mainly cytoplasmic, but members of this family are also present in other cellular compartments, such as the nucleus, mitochondria, and Golgi apparatus (*16*, *19*, *22*). A recent report suggests that 14-3-3 proteins transit to the nucleus and participate in nucleocytoplasmic transport in unsynchronized human osteosarcoma U2OS cells (*23*). 14-3-3 proteins are involved in many cellular mechanisms such as cell cycle control, mitogenic signal transduction, apoptotic cell death, acting as an adapter or chaperone element, and in the formation of complex cross-talks between proteins. The degree of complexity in the regulation of 14-3-3 functions is due to the large number of proteins that interact with this family. Raf, protein kinase C, mouse polyomavirus middle T antigen, Bcr, phosphoinositide 3-kinase, and Cdc25 are just a few examples of all reported 14-3-3 binding proteins (*24*, *25*).

† Work supported by the Cancer Research Society, Inc. (Grants to M.Z-H. and G.B.P.).

* Corresponding author. Phone: (514) 398-3536. Fax: (514) 398-6769. E-mail: maria.zannis@mcgill.ca.

‡ Department of Biochemistry.

§ Cancer Center.

[1] Abbreviations: AB, acrylamide:bisacrylamide; ARS, autonomous replication sequence; BN−PAGE, blue native polyacrylamide gel electrophoresis; BPB, bromophenol blue; Cas, Crk-associated factor; CBP, cruciform binding protein; DTT, dithiothreitol; ECL, enhanced chemiluminescence; EDTA, ethylenediaminetetraacetic acid; EMSA, electromobility shift assay; FACS, fluorescence-activated cell sorting; FBS, fetal bovine serum; IP, immunoprecipitate; IR, inverted repeat; NE, nuclear extracts; NRS, normal rabbit serum; O/N, overnight; pBS, pBluescript KS+; PC-F_{TH}, pre-cleared F_{TH}; PKC, protein kinase C; PMSF, phenylmethylsulfonyl fluoride; r14-3-3ζ-MBP, recombinant 14-3-3ζ tagged with maltose binding protein; r.t., room temperature; SDS−PAGE, sodium dodecyl sulfate polyacrylamide gel electrophoresis; s-s, serum-starved; WCE, whole cell extracts.

10.1021/bi027343p CCC: $25.00
Published on Web 05/17/2003

The first study implicating the 14-3-3 family in the binding to a biomolecule other than proteins, such as DNA, was that by Todd et al. (*16*). By sequencing of isolated tryptic peptides, it was shown that the 70 kDa polypeptide, which by Southwestern blot analysis was found specifically cross-linked to cruciform DNA, belonged to the 14-3-3 family.

Seven mammalian 14-3-3 isoforms have been identified (β, γ, ϵ, ζ, η, τ, and σ), which can dimerize via their conserved N-terminal region, forming homo- and heterodimeric combinations, a feature that allows this family to coordinate multiple pathways within the cell (*17*, *26*−*29*). The ζ and τ mammalian isoforms have been crystallized as dimers (*17*, *30*). A specific repertoire for dimerization between different 14-3-3 isoforms has been suggested (*28*), and evidence is accumulating, indicating that 14-3-3 isoforms do not dimerize randomly (*28*−*32*). Upon dimerization, 14-3-3 proteins form a groove, which has been proposed to be the cruciform DNA binding domain (*15*).

In the present study, we analyzed the cruciform binding activity of bacterially produced recombinant 14-3-3ζ bearing an N-terminus maltose binding protein tag (r14-3-3ζ-MBP) and its effect on mammalian in vitro DNA replication. The r14-3-3ζ-MBP was found to have CBP activity only when preincubated with F_{TH}, a CBP-enriched flow through fraction eluted by passage of HeLa cell total extracts first through DEAE Sephadex and then through a heparin column (*14*). Both r14-3-3ζ-MBP and endogenous 14-3-3ζ heterodimerized with the endogenous 14-3-3 isoforms β and ϵ, but not with the γ or σ isoforms, and addition of r14-3-3ζ-MBP in a mammalian in vitro DNA replication system resulted in an increase of p186 replication.

EXPERIMENTAL PROCEDURES

Cloning, Expression, and Factor XA Digestion of Recombinant 14-3-3ζ. The cDNA of 14-3-3ζ (kindly provided by Dr. Aitken, University of Edinburgh, Scotland) was cloned in the polylinker region of the plasmid pmal-c2X (New England Biolabs), which produces maltose-binding fusion proteins, using EcoR1 and Xba1 restriction sites. The rest of the procedure was followed as previously described (*31*). The r14-3-3ζ-MBP, in which the MBP tag is at the amino terminal end of the 14-3-3ζ protein, was eluted from the amylose column with either elution buffer [20 mM Tris-HCl, 200 mM NaCl, 1 mM ethylenediaminetetraacetic acid (EDTA), 10 mM maltose] or F_{TH} buffer (*14*) [0.01 M KH_2PO_4 pH 7.4, 0.15 M NaCl, 2.5 mM EDTA, 1 mM phenylmethylsulfonyl fluoride (PMSF), 1 Complete minitablet (Roche) per 10 mL of buffer solution] containing 10 mM maltose. A high degree of purity was detected in several fractions by a 12% sodium dodecyl sulfate polyacrylamide gel electrophoresis (SDS−PAGE) followed by Coomasie brilliant blue staining (data not shown). Approximately 2 mg of fusion protein was mixed with 20 μg of Factor XA (New England Biolabs) and incubated for 20 h at room temperature (r.t.). The digestion mix or equal amount of F_{TH} (as positive control) were loaded onto the amylose column. While F_{TH} was collected in the unbound fractions, the digestion products were collected with elution buffer. Also, F_{TH} was loaded onto an amylose column that had been previously loaded with r14-3-3ζ-MBP, the F_{TH} was flowed through, and the r14-3-3ζ-MBP eluted with elution buffer.

BN−*PAGE.* A blue native polyacrylamide gel electrophoresis (BN−PAGE) was performed by preparing a 4−13% acrylamide:bisacrylamide (AB) gradient with a 4% stacking gel. r14-3-3ζ-MBP before and after Factor XA digestion and r14-3-3ζ-MBP preincubated with F_{TH} during different periods of time (0, 2, 3, 9, and 18 h) were mixed with 1X native loading dye sample buffer [77 mM Tris-HCl pH 6.9, 15.3% glycerol, 0.012% bromophenol blue (BPB)]. Electrophoresis was performed at 100 V until BPB reached the separating gel and then at 500 V until BPB ran off the gel. The cathode buffer (50 mM Tricine, 15 mM Bis-Tris, 0.02% Coomasie blue G-250, pH 7 at 4 °C) was replaced by the same buffer containing no Coomasie blue dye when the BPB was 1/3 of the way into the separating gel. The gel, in which r14-3-3ζ-MBP before and after Factor XA digestion was loaded, was destained and photographed, whereas the gel, in which the r14-3-3ζ-MBP/F_{TH} mixtures were loaded, was transferred to Immobilon-P membrane (Millipore) at 100 V for 1 h at 4 °C, and the membrane was probed with anti-MBP antibody.

Analytical and Preparative Electromobility Shift Assays (EMSA). EMSAs were carried out as previously described (*14*−*16*, *18*, *19*), with some modifications. For analytical assays, increasing amounts (1, 10, and 100 ng) of pure r14-3-3ζ-MBP eluted with either elution buffer or F_{TH} buffer, Factor XA digestion products (10, 100, and 1000 ng), or 5 μg of F_{TH} that had been passed through the amylose column (positive control) were incubated with 0.3 ng of ^{32}P-labeled cruciform DNA (*14*) in the presence of the Elborough buffer (*33*) [20 mM Tris-HCl pH 7.5, 1 mM 1,4-dithiothreitol (DTT), 1 mM EDTA, 3% glycerol] and 100 ng/μL of poly-dI-dC (Pharmacia) for 0.5 h at 4 °C. The mixtures were subjected to 4% PAGE for 1.5 h at 180 V and r.t. in 1X TBE buffer. The gels were dried and exposed for autoradiography O/N.

For preparative EMSAs, a similar protocol was followed. 500 μg of F_{TH} was preincubated with either 100 ng of pure r14-3-3ζ-MBP or elution buffer at 4 °C O/N, and either of these mixtures or 500 μg of freshly prepared F_{TH} (not preincubated O/N) were then reacted with 50 ng of ^{32}P-labeled cruciform DNA (*14*) in Elborough buffer (*33*) and 100 ng/mL of poly-dI-dC for 0.5 h on ice. The reaction mixtures were loaded on a 4% polyacrylamide gel and subjected to electrophoresis at 180 V for 1.5 h, and the gel was wet-exposed O/N. The two bands corresponding to the CBP−cruciform DNA complexes were excised from the gel, subjected to isotachophoresis (*15*), concentrated with a YM-10 concentrator (QIAGEN) to a final concentration of approximately 0.5 μg/μL, and mixed with 1X SDS loading sample buffer (50 mM Tris-HCl, 100 mM DTT, 2% SDS, 0.1% BPB, 10% glycerol). The same procedure was followed for mixtures of r14-3-3ζ-MBP (100 ng) and F_{TH} (500 μg) that were preincubated for 0, 2, 3, 9, and 18 h.

Immunoprecipitation with Anti-MBP and Anti-14-3-3ζ *Antibodies.* Approximately 500 μg of F_{TH} was precleared (PC) with 30 μL of Protein-A agarose by incubation for 3 h at 4 °C and centrifuged for 5 min at 1500*g*. 2 μg of r14-3-3ζ-MBP was added to 2/3 of the supernatant (PC-F_{TH}) and incubated at 4 °C O/N; the remaining 1/3 of the PC-F_{TH} was kept as control. Either 5 μg of anti-MBP antibody or same amount of normal rabbit serum (NRS) was added to half portions of PC-F_{TH} + r14-3-3ζ-MBP, and the mixtures were incubated for 3 h at 4 °C, followed by addition of 15 μL of

Protein-A agarose and a further incubation for 3 h. The mixtures were centrifuged for 5 min at 1500*g* at 4 °C. The immunoprecipitate (IP) was washed with RIPA buffer [1% Nonidet P-40, 5% sodium deoxycholate, 0.1% SDS, 0.1 mM of PMSF, and 1 Complete Minitablet (Roche) per 10 mL of buffer solution] three times and finally resuspended in 1X SDS sample buffer. Similarly, nuclear extracts (NE) prepared from 2×10^7 HeLa cells from each s-s, G_1/S, and G_2/M cultures were processed as described above prior to incubation with either 1 μg of anti-14-3-3ζ antibody or the same amount of NRS. IPs were collected, washed, and resuspended as described above.

SDS−PAGE and Western Blotting. 36 μL of band-shift eluted CBP−cruciform DNA complexes; r14-3-3ζ-MBP eluted before and after F_{TH} was flowed through the column loaded with r14-3-3ζ-MBP, anti-MBP, or anti-14-3-3ζ antibodies IPs, and HeLa whole cell extracts (WCE) or NE were mixed with 1X SDS sample buffer and loaded on a 12% SDS polyacrylamide gel. Electrophoresis was carried out at 100 V for 20 min and then at 200 V for 30 min. The contents on the gels were electrotransferred to Immobilon-P membrane (Millipore) at 100 V for 1 h at 4 °C, and the membranes were probed with anti-MPB (New England Biolabs), anti-14-3-3ζ (Santa Cruz Biotechnology; SC 1019), anti-14-3-3β (SC 628), anti-14-3-3γ (SC 731), anti-14-3-3ϵ (SC 1020), anti-14-3-3σ (SC 7681), anti-14-3-3 pan antibody (SC 1657), anti-Cas/p130 (SC 860), anti Crk II (SC 289), and anti-Orc2 (kindly provided by Dr. Bruce Stillman, Cold Spring Harbor Laboratory, NY) antibodies. Protein−antibody complexes were visualized by enhanced chemiluminescence (ECL) using the Amersham ECL system, with goat anti-rabbit (or anti-goat in the case of anti-14-3-3σ blots) horseradish-peroxidase (HRP)-labeled conjugated secondary antibody (Santa Cruz Biotechnology).

HeLa Cell Culture and Synchronization. HeLa cells (monolayers) were cultured in MEMα medium (Gibco-BRL, NY) supplemented with 10% fetal bovine serum (FBS, Gibco-BRL) at 37 °C and were either serum-starved or blocked at the G_1/S or G_2/M phases, as previously described (*18*, *19*, *34*) with some modifications. Log phase cells at 80% confluence were serum-starved for 48 h and collected as G_0 phase cells (hereafter termed serum-starved, or s-s, cells). Log phase cells at 50% confluence were also serum-starved for 48 h, then 10% serum and 2 mM thymidine were added, and the cells were further incubated at 37 °C for 12 h. The thymidine-based medium was then replaced by normal medium with 10% FBS, and the cells were further incubated at 37 °C for 9 h. For G_1/S synchronization, the cells (hereafter termed G_1/S cells) were placed in normal medium, containing 10% FBS and 10 mM hydroxyurea for 12 h, while for G_2/M synchronization cells (hereafter termed G_2/M cells) were placed in normal medium containing 10% FBS and 1 μg/mL nocodazole. Synchronization was monitored by fluorescence-activated cell sorting (FACS) analysis.

Preparation of HeLa Whole Cell Extract (WCE) and Nuclear Extract (NE). HeLa WCE and NE were prepared as described in (*35*), with some modifications. In brief, for WCE, approximately 10^7 cells were harvested by centrifugation at 4 °C, resuspended in 1X SDS sample buffer to a concentration of 2.8×10^4 cells/μL, and sonicated at a 40% amplitude for three periods of 30 s each, with resting periods of 1 min in between. For NE, approximately 10^7 cells were harvested by centrifugation at 4 °C and lysed in hypotonic buffer (20 mM Hepes-KOH pH 8.0, 5 mM KCl, 1.5 mM $MgCl_2$, 5 mM Na butyrate, and 0.1 mM DTT) with a 21G1 needle. Nuclei were collected by centrifugation at 16 000*g* for 10 min at 4 °C, washed three times with hypotonic buffer and resuspended in nuclear extraction buffer (15 mM Tris-HCl pH 7.5, 1 mM EDTA, 0.4 M NaCl, 10% sucrose, and 1 mM DTT), incubated at 4 °C for 0.5 h, and centrifuged at 100 000*g* for 40 min at 4 °C. The supernatant (soluble nuclear proteins) was mixed with 1X SDS sample buffer to a concentration of 2.8×10^4 cells/μL (or 2.8×10^4 nuclei/μL).

In Vitro DNA Replication. In vitro DNA replication assays were performed as previously described (*18*, *19*, *36*) with some modifications. In brief, approximately 150 μg of HeLa WCE were preincubated for 3 h with elution buffer, or 0.75, 1.5, or 7.5 μg of r14-3-3ζ-MBP, or the same respective equimolar amounts of MBP. Approximately 150 ng of p186 template DNA (*18*, *19*, *37*) and the rest of the reaction ingredients were added, and the mixtures were incubated for 1 h at 30 °C. In addition, 100 ng of unmethylated pBluescript KS+ (pBS) was added to each reaction to internally control for differences in DNA recovery and DpnI digestion (*18*, *19*). The replication products were purified by passing them through QIAquick PCR Purification Kit columns (QIAGEN), and 1/3 of each sample was digested with 1.5 U of DpnI (New England BioLabs), as described previously (*18*, *19*, *38*) for 1 h at 37 °C. Both undigested and digested products were resolved by electrophoresis in a 1% agarose gel for 15 h at 55 V, the dried gel was exposed to an imaging plate for 5 h, and the DpnI resistant bands corresponding to the plasmid DNA forms II and III were quantified by Image Gauche (Fuji Photo Film Co., Ltd.), as previously described (*18*, *19*, *38*). The optimal amount (units) of DpnI required for the digestion reactions was determined as previously described (*19*).

RESULTS

Pure r14-3-3ζ-MBP Does Not Have Cruciform DNA Binding Activity. The cruciform binding (CBP) activity of pure r14-3-3ζ-MBP protein was tested by analytical EMSA, as previously described (*14*−*16*, *18*, *19*). Following incubation of increasing amounts (1, 10, and 100 ng) of r14-3-3ζ-MBP eluted in elution buffer with end-labeled cruciform DNA in the presence of DNA binding buffer, no band-shift was observed (Figure 1, lanes 2−4), by comparison to the migration of free cruciform DNA (Figure 1, lane 1). Similarly, no band-shift was observed when the same amounts of r14-3-3ζ-MBP that was eluted with F_{TH} buffer were reacted with cruciform DNA (Figure 1, lanes 6−8). In contrast, the two regular band-shifted complexes (*14*, *16*) were observed when cruciform DNA was incubated with the human CBP-enriched fraction (F_{TH}), used as positive control (Figure 1, lane 5). These results suggested that either pure r14-3-3ζ-MBP was not active because the MBP tag interfered with its dimerization domain or that it was inactive by itself and required heterodimerization with an endogenous 14-3-3 isoform to be activated as a cruciform binding protein.

r14-3-3ζ-MBP Digested by Factor XA Does Not Bind Cruciform DNA. To analyze whether the presence of the MBP moiety at the N-terminus of r14-3-3ζ-MBP interfered

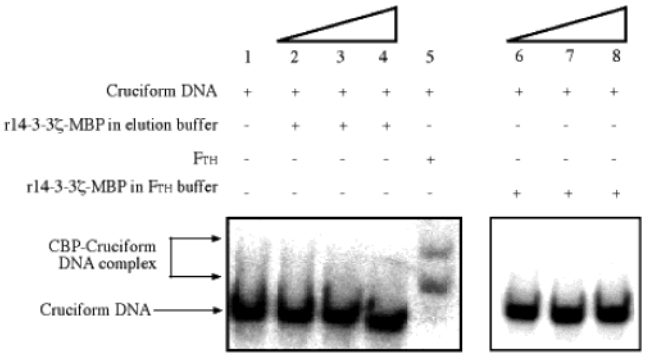

FIGURE 1: Pure r14-3-3ζ-MBP does not have cruciform DNA binding activity. Increasing amounts (1, 10, and 100 ng) of pure r14-3-3ζ-MBP elute with either elution buffer (lanes 2−4) or F_{TH} buffer (lanes 6−8) were subjected to EMSA by reacting with labeled cruciform DNA (arrow; lane 1). Five μg of F_{TH} was used as positive control (lane 5), and the formation of the CBP−cruciform DNA complexes is indicated (double arrow).

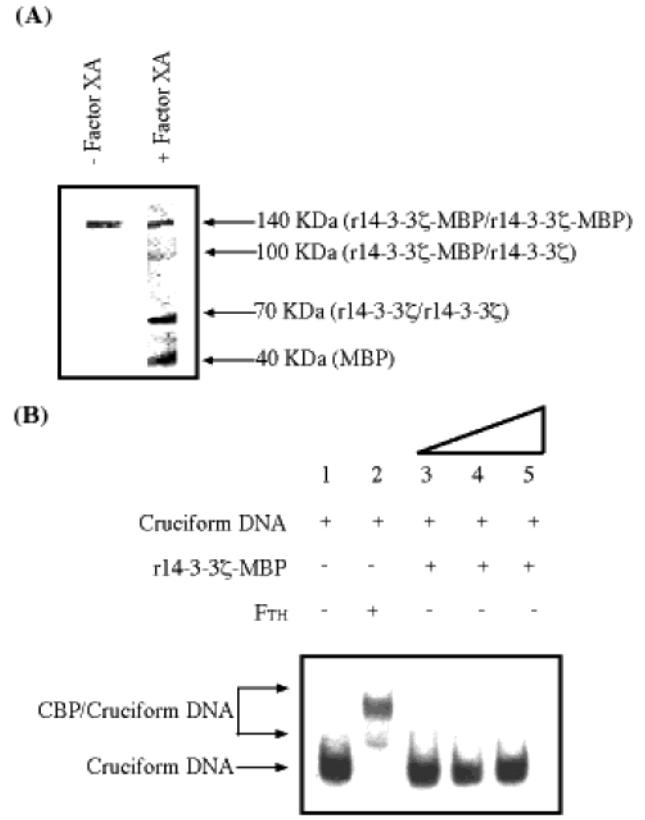

FIGURE 2: Pure r14-3-3ζ-MBP can dimerize but has no cruciform DNA binding activity. (A) Approximately 2 mg of r14-3-3ζ-MBP (−Factor XA) was digested with Factor XA (+Factor XA), and the digestion products were resolved by BN−PAGE. The consistency and molecular weight of the digestion products are indicated (arrows). (B) Increasing amounts of Factor XA digestion products (10 ng, lane 3; 100 ng, lane 4; and 1000 ng, lane 5) were reacted with labeled cruciform DNA (arrow; lane 1) and subjected to EMSA on a 4% polyacrylamide gel. Five μg of F_{TH} that had been flowed through the amylose column was used as positive control (lane 2). The position of the CBP−cruciform DNA complexes is indicated (double arrow).

with r14-3-3ζ-MBP/r14-3-3ζ-MBP homodimer formation, pure r14-3-3ζ-MBP was subjected to BN−PAGE before and after digestion by Factor XA, which digests the MBP tag of the recombinant protein. The results (Figure 2A) show that only one band of approximately 140 kDa was present before Factor XA digestion (−Factor XA lane), indicating that almost 100% of the recombinant protein was present in dimer form (r14-3-3ζ-MBP/r14-3-3ζ-MBP). Following digestion with Factor XA (Figure 2A, +Factor XA lane), four bands could be detected: a band of approximately 140 kDa, corresponding to the dimeric undigested form of r14-3-3ζ-MBP; a faint band of approximately 100 kDa, corresponding to the dimeric r14-3-3ζ-MBP with one of the MBP tags uncut (r14-3-3ζ-MBP/r14-3-3ζ); a band of approximately 66 kDa, corresponding to the dimeric r14-3-3ζ with both of the MBP tags removed (r14-3-3ζ/r14-3-3ζ); and a band of approximately 40 kDa, corresponding to monomeric MBP protein. These results indicate that r14-3-3ζ-MBP was somewhat resistant to Factor XA digestion, that r14-3-3ζ/r14-3-3ζ homodimer was produced, and that the MBP tag did not interfere with the formation of the r14-3-3 dimer.

To ascertain whether the Factor XA enzymatic action produced at least one active cruciform binding protein combination, increasing amounts (10, 100, and 1000 ng) of the purified digestion products were subjected to EMSA analysis in DNA binding buffer. No band-shift was observed (Figure 2B, lanes 3−5), by comparison to the migration of free cruciform DNA (Figure 2B, lane 1), indicating the absence of cruciform binding activity from the Factor XA digestion mix. In contrast, F_{TH} collected from the amylose column produced the expected CBP−cruciform DNA complexes (Figure 2B, lane 2).

r14-3-3ζ-MBP Binds to Cruciform DNA After Preincubation with F_{TH}. In view of the recent finding that the two *Saccharomyces cerevisiae* 14-3-3 homologues, Bmh1p and Bmh2p, require heterodimerization to exhibit strong cruciform binding activity (*21*), we tested the ability of r14-3-3ζ-MBP to heterodimerize with endogenous 14-3-3 isoforms present in F_{TH} and in this manner attain cruciform binding activity. For this, F_{TH} was preincubated with either pure r14-3-3ζ-MBP or elution buffer (O/N, 4 °C), and the mixtures were then incubated with labeled cruciform DNA (20 min, 4 °C) and analyzed by preparative EMSA. Freshly prepared F_{TH} was used as positive control for the O/N preincubation and further EMSA and immunoblotting reactions. In each case (Figure 3A) (i.e., when F_{TH} preincubated with r14-3-3ζ-MBP (lane 2), with elution buffer only (F_{TH} preincubated; lane 3), or not preincubated at all (freshly prepared F_{TH}; lane 4) was used), a band-shift was observed, indicating the formation of the CBP−cruciform DNA complex, by comparison to the migration of free cruciform DNA (Figure 3A, lane 1). These three complexes (Figure 3A, lanes 2−4) were isolated by isotachophoresis (*15*), subjected to SDS−PAGE, and immunoblotted with either anti-14-3-3ζ antibody (Figure 3B) or anti-MBP antibody (Figure 3C). When the immunodetection was performed with anti-14-3-3ζ antibody, the three complexes were found to contain endogenous 14-3-3ζ (Figure 3B, lanes 2−4), as specific bands of approximately 30 kDa were detected. The same antibody also detected an extra specific band at approximately 70 kDa (Figure 3B, lane 2), corresponding to the fusion protein 14-3-3ζ-MBP. This band, however, was not present in the CBP−cruciform DNA complex from the control reactions, either when F_{TH} was preincubated with elution buffer only (Figure 3B, lane 3) or when the complex was formed from freshly prepared F_{TH} (Figure 3B, lane 4). The 70 kDa band detected with anti-14-3-3ζ antibody was also detected with anti-MBP antibody

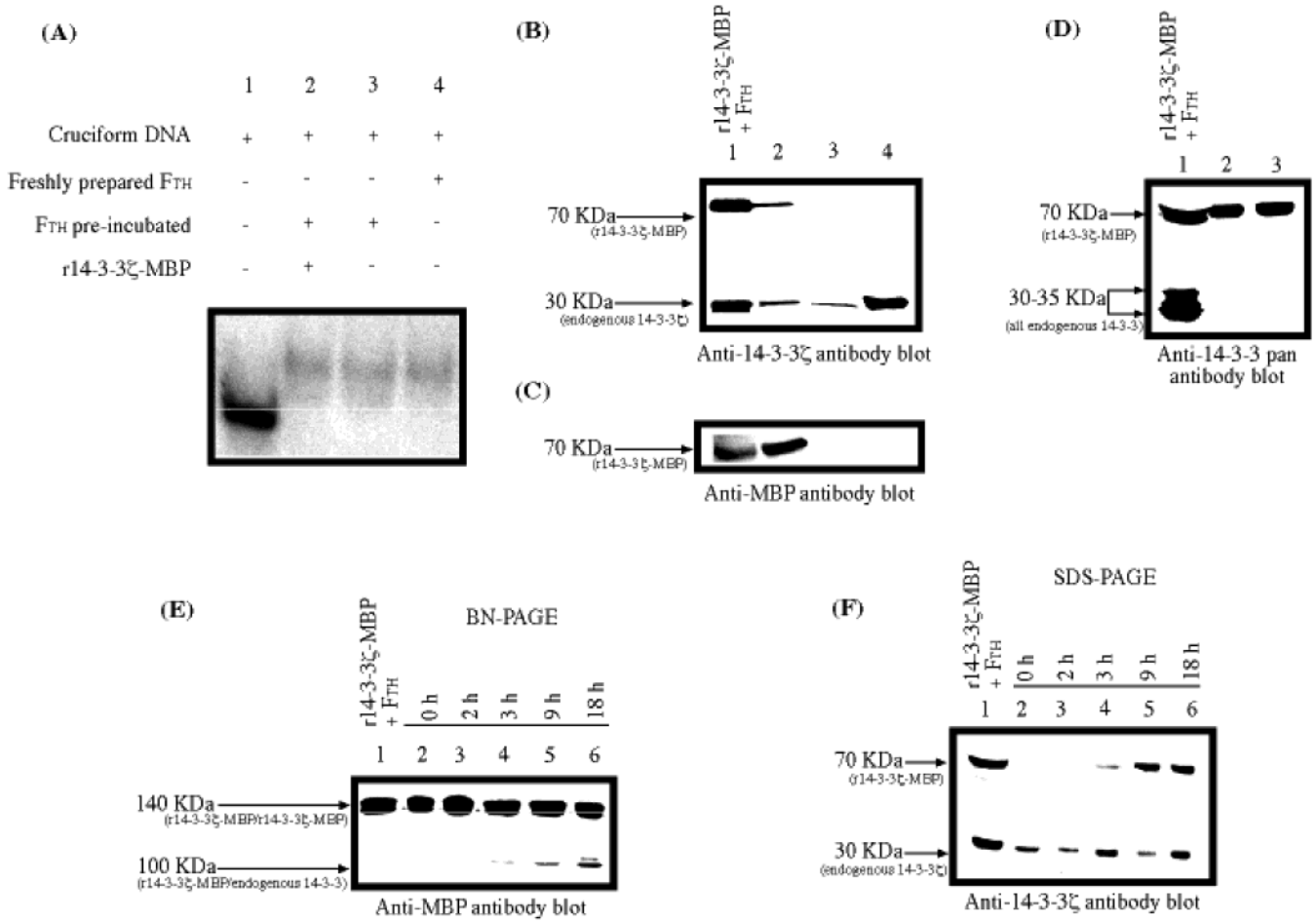

FIGURE 3: Pure r14-3-3ζ-MBP binds to cruciform DNA after preincubation (O/N, 4 °C) with CBP enriched fraction (F_{TH}). (A) A 4% polyacrylamide gel EMSA showing three CBP−cruciform DNA complexes detected after reacting labeled cruciform DNA (lane 1) with F_{TH} preincubated with either r14-3-3ζ-MBP (lane 2) or with elution buffer only (lane 3), or with freshly prepared F_{TH} (lane 4). The three CBP−cruciform DNA complexes (lanes 2−4) were excised from the gel and subjected to isotachophoresis followed by SDS−PAGE and Western blot analysis with (B) anti-14-3-3ζ and (C) anti-MBP antibody. The r14-3-3ζ-MBP (70 kDa; lanes 1 and 2) and the endogenous 14-3-3ζ (30 kDa; lanes 1−4) protein monomers are indicated (arrow). (D) SDS−PAGE followed by Western blot analysis, with an anti-14-3-3 pan-antibody, of r14-3-3ζ-MBP eluted from an amylose column before (lane 2) and after (lane 3) passage of F_{TH} through the column. The position of the r14-3-3ζ-MBP (arrow) and all endogenous 14-3-3 isoforms (double arrow) in the positive control (lane 1) are indicated. F_{TH} was preincubated with r14-3-3ζ-MBP for 0, 2, 3, 9, and 18 h (lanes 2−6, respectively) before being subjected to either (E) BN−PAGE followed by Western blot analysis with anti-MBP antibody or (F) SDS−PAGE followed by Western blot analysis with anti-14-3-3ζ antibody. A r14-3-3ζ-MBP/F_{TH} mixture was used as positive control (lane 1). The position of the r14-3-3ζ-MBP/r14-3-3ζ-MBP homodimer and the r14-3-3ζ-MBP/endogenous 14-3-3 heterodimers in the BN−PAGE and the r14-3-3ζ-MBP and endogenous 14-3-3ζ in the SDS−PAGE are indicated (arrow).

(Figure 3C, lane 2) but not in the other two isolated complexes (Figure 3C, lanes 3 and 4), confirming the presence of r14-3-3ζ-MBP in the CBP−cruciform DNA complex. As a positive control for immunoblotting, a mixture of F_{TH} and r14-3-3ζ-MBP was immunoblotted with both anti-14-3-3ζ and anti-MBP antibodies, and both endogenous and recombinant proteins were detected (Figure 3B,C, lane 1), as expected.

Parallel to the three complexes that were isolated from Figure 3A, r14-3-3ζ-MBP protein alone was also subjected to electrophoresis in the same acrylamide gel (data not shown). The region of the gel corresponding to the CBP−cruciform DNA complex was excised from this lane and subjected to isotachophoresis (*15*), followed by SDS−PAGE and Western blot analysis with anti-MBP antibody. No r14-3-3ζ-MBP was detectable at this position of the gel, indicating that r14-3-3ζ-MBP was present in the cruciform DNA−CBP complex (Figure 3A−C, lane 2) because it was bound to cruciform DNA (data not shown). To determine whether endogenous 14-3-3 isoforms were simply sticking to r14-3-3ζ-MBP in a loose association and not heterodimerizing with it, r14-3-3ζ-MBP was eluted from the amylose column before (Figure 3D, lane 2) and after (Figure 3D, lane 3) passage of F_{TH} through the column, where r14-3-3ζ-MBP had been previously bound, and subjected to SDS−PAGE and Western blot analysis with an anti-14-3-3 pan antibody. No band corresponding to endogenous 14-3-3 isoform was detected in either eluate (lanes 2 and 3) as compared to the positive control, a mixture of F_{TH} and r14-3-3ζ-MBP (Figure 3D, lane 1).

To analyze the kinetics with which the 14-3-3 dimers exchange partners (i.e., how fast r14-3-3ζ-MBP homodimers dissociate and associate with endogenous 14-3-3 isoforms) and whether at the same time r14-3-3ζ-MBP acquires cruciform binding activity, F_{TH} was incubated with r14-3-3ζ-MBP for 0, 2, 3, 9, or 18 h, and the mixtures were then subjected to either BN−PAGE followed by immunodetection with anti-MBP antibody (Figure 3E) or preparative EMSA

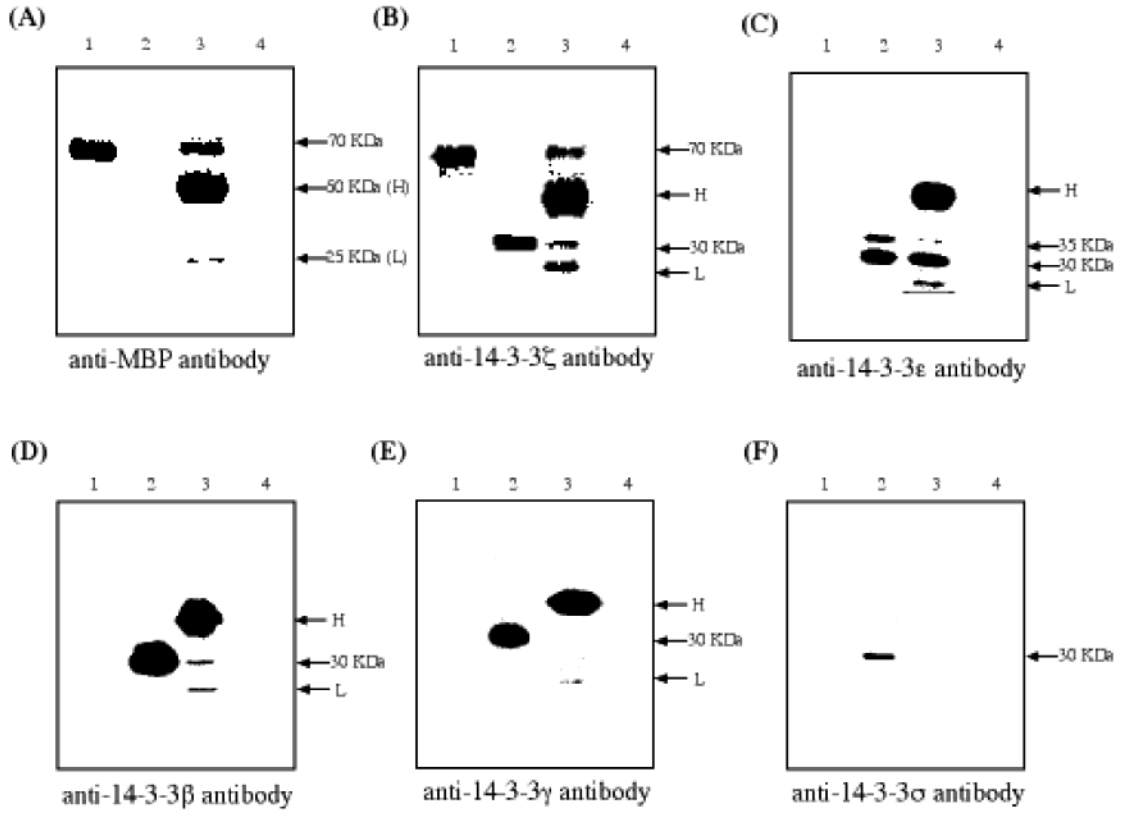

FIGURE 4: r14-3-3ζ-MBP dimerizes with endogenous 14-3-3β, ϵ, and ζ isoforms. Western blot analysis of immunoprecipitate (IP) obtained with either anti-MBP antibody (lane 3) or NRS (lane 4) from F_{TH} preincubated with r14-3-3ζ-MBP (A−F). (A) Anti-MBP; (B) anti-14-3-3ζ; (C) anti-14-3-3ϵ; (D) anti-14-3-3β; (E) anti-14-3-3γ; and (F) anti-14-3-3σ. The presence of r14-3-3ζ-MBP (70 kDa; panels A and B, lane 3), endogenous 14-3-3ζ (30 kDa; panel B, lane 3), 14-3-3ϵ (30 kDa; panel C, lane 3), and 14-3-3β (30 kDa; panel D, lane 3) protein monomers in the anti-MBP antibody IP are indicated (arrow). The absence of 14-3-3γ (panel E, lane 3) and 14-3-3σ (30 kDa; panel F, lane 3) protein monomers from the anti-MBP antibody IP is also indicated (arrow). The heavy (H) and light (L) chains of the anti-MBP antibody are indicated (arrows; panels A−E). r14-3-3ζ-MBP (all panels, lane 1) and precleared F_{TH} (all panels, lane 2) were used as positive control for immunodetection.

(data not shown) followed by electroelution of the CBP−cruciform DNA complexes, SDS−PAGE, and immunodetection with anti-14-3-3ζ antibody (Figure 3F). In the 0- and 2-h incubation mixtures, only the r14-3-3ζ-MBP/r14-3-3ζ-MBP homodimer was detected, as evidenced by the presence of a single band of approximately 140 kDa (Figure 3E, lanes 2 and 3), whereas in the 3-, 9-, and 18-h incubation mixtures, a band of approximately 100 kDa was also present, in addition to the 140-kDa band (Figure 3E, lanes 4−6), indicating the presence of r14-3-3ζ-MBP/endogenous 14-3-3 heterodimers. Similarly, the presence of r14-3-3ζ-MBP in the CBP−cruciform DNA complex was detected only after a 3-h incubation of F_{TH} with r14-3-3ζ-MBP (Figure 3F, lanes 4−6), as the approximately 70-kDa band corresponding to the r14-3-3ζ-MBP was only present in the complexes isolated from the 3-, 9-, and 18-h incubation reactions. Again, a mixture of r14-3-3ζ-MBP with F_{TH} was used as a control for the Western blot analyses (Figure 3E,F, lane 1).

r14-3-3ζ-MBP Heterodimerizes with Endogenous 14-3-3 Isoforms β, ϵ, and ζ. To confirm that r14-3-3ζ-MBP was able to heterodimerize with endogenous 14-3-3 isoforms present in F_{TH}, thus attaining cruciform binding activity, an immunoprecipitation with anti-MBP antibody was performed using the F_{TH} fraction that was preincubated with r14-3-3ζ-MBP, followed by immunodetection with antibodies specific for each of the 14-3-3 isoforms (β, γ, ϵ, ζ, and σ) and for MBP. The results (Figure 4) show that in the anti-MBP antibody immunoprecipitation (Figure 4A), a specific band of approximately 70 kDa was detected, corresponding to the recombinant protein (Figure 4A, lane 3). Two other bands were also detected when anti-rabbit antibody was used as the secondary antibody, corresponding to the heavy (H; 50 kDa) and light (L; 25 kDa) chains of the anti-MBP antibody present in the IP (Figure 4A−E, lane 3). These bands were not detected when anti-goat antibody was used as secondary antibody (Figure 4F, lane 3). The r14-3-3ζ-MBP protein was used as positive control for the immunodetection performed with anti-MBP antibody (Figure 4A,B, lane 1). Likewise, precleared F_{TH} (PC-F_{TH}) was used as control for the presence of the 14-3-3 isoforms, against which specific immunodetection was performed, and all five isoforms were detected with their respective antibodies in this fraction, unlike MBP, which was absent (Figure 4B−F, lane 2). The presence of r14-3-3ζ-MBP in the IP was further confirmed by immunoblotting with anti-14-3-3ζ antibody, where an approximately 70-kDa band (corresponding to the fusion recombinant protein) and an approximately 30-kDa band (corresponding to the 14-3-3ζ monomer) were detected (Figure 4B, lane 3), indicating that r14-3-3ζ-MBP was able to heterodimerize with the endogenous 14-3-3ζ isoform. Similarly, when the immunodetection was carried out with anti-14-3-3ϵ and anti-14-3-3β antibodies, a specific band of approximately 30 kDa could be detected (Figure 4C,D, lane 3), indicating that the ϵ and β isoforms were also able to heterodimerize with r14-

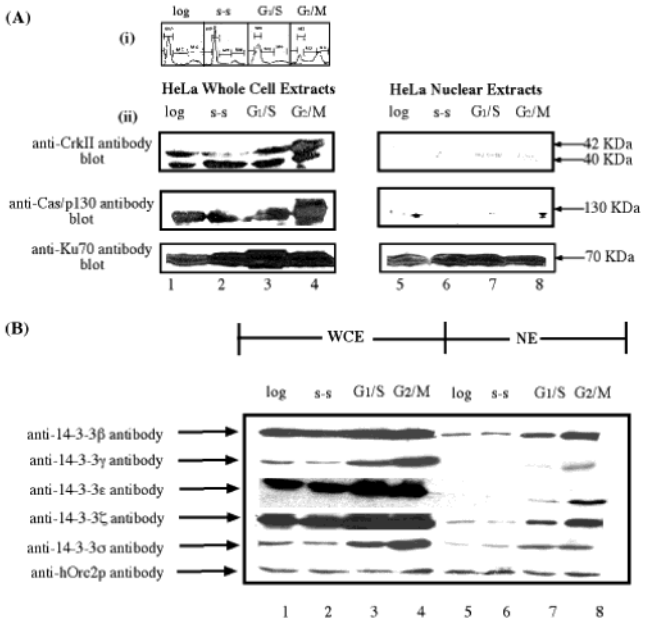

FIGURE 5: Cell cycle-dependent expression and nuclear presence of 14-3-3β, γ, ϵ, ζ, and σ isoforms. (A, part i) FACS analysis of HeLa cells at log phase and after serum-starvation (s-s) and block to G_1/S and G_2/M phases of the cell cycle; (part ii) Western blot of WCE and NE from s-s, G_1/S and G_2/M HeLa cells probed with anti-CrkII, anti-Cas/p130, and anti-Ku70 antibodies. The CrkII (40 and 42 kDa), Cas/p130 (130 kDa), and Ku70 (70 kDa) proteins are indicated (arrow). (B) Western blot of synchronized WCE and NE probed with anti-14-3-3β, γ, ϵ, ζ, and σ and with anti-hOrc2p antibodies; the position of the respective proteins is indicated (arrow).

3-3ζ-MBP. The extra band of approximately 35 kDa detected in the PC-F_{TH} with the anti-14-3-3ϵ antibody (Figure 4C, lane 2) has been previously detected and is characteristic of human CBP (*16*, *19*). In contrast, neither isoform γ (Figure 4E, lane 3) nor σ (Figure 4F, lane 3) were detected when the IP was immunoblotted with anti-14-3-3γ and anti-14-3-3σ antibodies, respectively, suggesting that neither of these isoforms was able to heterodimerize with r14-3-3ζ-MBP. None of the proteins (MBP or 14-3-3) was detected after immunoprecipitation with NRS (Figure 4A−F, lane 4).

Total 14-3-3 Protein Expression and Nuclear Presence Are Increased at G_1/S and G_2/M. To determine that endogenous nuclear 14-3-3ζ was also able to form heterodimers, as the recombinant form was able to do with the β and ϵ isoforms present in the F_{TH}, WCE and NE were prepared from HeLa cells that were either serum-starved (s-s) or blocked at the G_1/S or G_2/M phases of the cell cycle (Figure 5A (i)) and used to perform an anti-14-3-3ζ immunoprecipitation followed by SDS−PAGE and Western blot analyses, using anti-14-3-3β, γ, ϵ, ζ, and σ antibodies. FACS analysis (Figure 5A (i)) revealed that the distribution of cells that were blocked at G_1/S was approximately 55% in G_1, 23% in S, and 10% in G_2/M; while the distribution of cells blocked at G_2/M was 19% in G_1, 12% in S, and 44% in G_2/M; and that of s-s cells was 63% in G_1, 11% in S, and 15% in G_2/M. The NE prepared from these cells were tested for cytoplasmic contamination by immunoblotting with antibodies against two exclusively cytoplasmic proteins, CrkII (40 and 42 kDa) and Cas/p130 (130 kDa; ref *39*). Only trace amounts of both of these proteins were present in the NE prepared from each phase of the cell cycle (Figure 5A (ii), lanes 5−8; anti-CrkII and anti-Cas/p130 antibody blots), by comparison to the amount present in the WCE (Figure 5A (ii), lanes 1−4; anti-CrkII and anti-Cas/p130 antibody blots); less than 0.5% of the total intensity after immunodetection was calculated for each protein (data not shown). Furthermore, as a positive control for the Western blotting analysis, immunodetection with an antibody against Ku70, an abundant nuclear protein (ref *38* and refs therein), was preformed, and Ku70 was detected in all cell cycle phases in both WCE and NE (Figure 5A (ii), lanes 1−8; anti-Ku70 antibody blot). The WCE and NE prepared from s-s, G_1/S, and G_2/M cells were subjected to immunodetection analyses for the 14-3-3 isoforms β, γ, ϵ, ζ, and σ and the exclusively nuclear protein hOrc2p (*35*), using their respective antibodies (Figure 5B). When comparing the same number of cells, the total expression per cell of all these 14-3-3 isoforms was, in general, higher in the G_1/S and G_2/M cells (Figure 5B, lanes 3 and 4; all 14-3-3 blots), by comparison to their expression in the s-s cells (Figure 5B, lane 2; all 14-3-3 blots), as was their presence in the nucleus (Figure 5B, lanes 6−8; all 14-3-3 blots). In particular, the γ and ϵ isoforms were barely detectable in the NE from s-s cells (Figure 5B, lane 6; anti-14-3-3γ and anti-14-3-3ϵ antibody blots), whereas they were both readily detectable at G_1/S and G_2/M (Figure 5B, lanes 7 and 8; anti-14-3-3γ and anti-14-3-3ϵ antibody blots). Log phase WCE and NE, used as control for the immunodetection, gave similar results to those obtained with the s-s extracts (Figure 5B, lanes 1 and 5, respectively; all blots). The expression of Orc2p, also used as control, did not change throughout the cell cycle (Figure 5B, lanes 2−4; anti-hOrc2p antibody blot) and was always nuclear (Figure 5B, lanes 6−8; anti-hOrc2p antibody blot), consistent with previous observations (*35*). The quantification of these 14-3-3 isoforms in the nuclear extracts of the s-s, G_1/S, and G_2/M cells, calculated by band intensity and given in arbitrary units, is summarized in Table 1.

Endogenous 14-3-3ζ/β and 14-3-3ζ/ϵ Heterodimers Are Present in the Nucleus at G_1/S and G_2/M. An anti-14-3-3ζ antibody immunoprecipitation was performed from the NE of the s-s, G_1/S, or G_2/M HeLa cells. The results (Figure 6) showed that anti-14-3-3ζ antibody was able to immunoprecipitate the endogenous ζ isoform (Figure 6, lanes 2, 5, and 8; anti-14-3-3ζ antibody blot) from the s-s, G_1/S, and G_2/M NE (Figure 6, lanes 1, 4, and 7; anti-14-3-3ζ antibody blot). In contrast, although both the β and the σ isoforms were present in the s-s NE (Figure 6, lane 1; anti-14-3-3β and anti-14-3-3σ antibodies blots), only the β isoform was immunoprecipitated (not always reproducible) by the anti-14-3-3ζ isoform (Figure 6, lane 2; anti-14-3-3β antibody blot), whereas the σ isoform was not (Figure 6, lane 2; anti-14-3-3σ antibody blot), indicating that only the 14-3-3ζ/β heterodimer might be present in the s-s nucleus (Table 1). The 14-3-3ϵ isoform was not consistently detectable in the s-s NE (Table 1 and Figure 6, lane 1; anti-14-3-3ϵ antibody blot) and was not immunoprecipitated by the anti-14-3-3ζ antibody from this extract (Figure 6, lane 2; anti-14-3-3ϵ antibody blot), while the γ isoform was detected neither in the NE (Table 1 and Figure 6, lane 1; anti-14-3-3γ antibody blot) nor in the anti-14-3-3ζ antibody IP (Figure 6, lane 2; anti-14-3-3γ antibody blot) at the s-s stage. As the presence of the ϵ isoform increased by approximately 24-fold in G_1/S NE by comparison to s-s NE (Table 1 and Figure 6, lane 4;

Table 1: Amount[a] (Arbitrary Unit) of 14-3-3 Isoforms in HeLa Cell NE[b] from s-s, G_1/S, and G_2/M Cultures and Participation in Heterodimers[c] with the 14-3-3ζ Isoform

14-3-3 isoforms/ cycle phase	β	γ	ϵ	ζ	σ	hOrc2p
s-s	8.5 ± 1.5	0.16 ± 0.1	0.75 ± 0.3	2.9 ± 0.8	9.6 ± 3.1	15.6 ± 2.3
G_1/S	26.2 ± 3.4	4.5 ± 1.8	18.4 ± 2.1	27.5 ± 2.9	42.0 ± 5.8	17.1 ± 2.5
G_2/M	47.9 ± 4.2	12.8 ± 2.7	39.5 ± 4.3	68.4 ± 6.4	47.9 ± 6.4	17.7 ± 3.6
dimerization with ζ in s-s NE	±	−	−	N/D	−	N/D
dimerization with ζ in G_1/S and G_2/M	+	−	+	N/D	−	N/D

[a] The amount of the 14-3-3 isoforms (β-σ) corresponds to the Western blot band intensity quantified by Image Gauche (Fuji Photo Film Co., LTD) and therefore is given in arbitrary units. The amount of HOrc2p in the nucleus at the three phases was used as a control. [b] Nuclear extracts (NE) prepared from s-s, G_1/S, and G_2/M HeLa cell cultures were subjected to SDS−PAGE, followed by Western blot analysis with anti-14-3-3β, γ, ε, ζ, and σ antibodies. [c] + indicates heterodimerization of these isoforms with 14-3-3ζ; − indicates that these isoforms were not found in heterodimers with 14-3-3ζ; N/D indicates not determined.

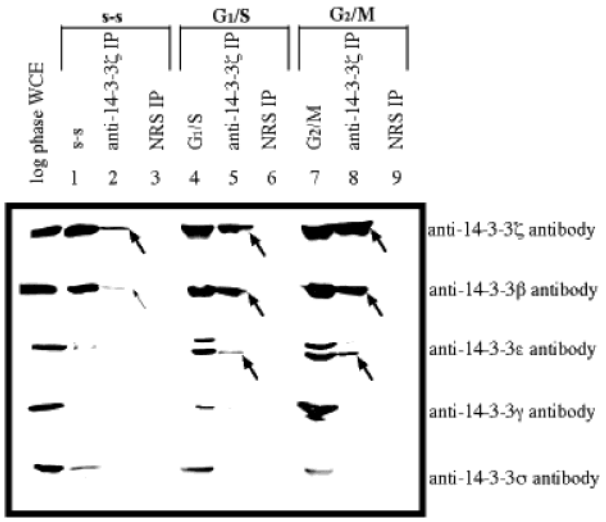

FIGURE 6: Cell cycle-dependent nuclear presence of 14-3-3ζ/β and 14-3-3ζ/ε heterodimers. NE from s-s (lane 1), G_1/S (lane 4), and G_2/M (lane 7) HeLa cells were immunoprecipitated with either anti-14-3-3ζ antibody (lanes 2, 5, and 8) or NRS (lanes 3, 6, and 9), and the IPs were probed with anti-14-3-3ζ, anti-14-3-3β, anti14-3-3ε, anti-14-3-3γ, and anti-14-3-3σ antibodies. The ζ, β, and ε isoforms (arrows) in the anti-14-3-3ζ antibody IP from G_1/S and G_2/M NE and the ζ (arrow) and β (light arrow) isoforms in the anti-14-3-3ζ antibody IP from s-s NE are indicated. The log phase WCE lane represents the positive control for immunodetection.

anti-14-3-3ε antibody blot), it was also immunoprecipitated from the G_1/S NE by the anti-14-3-3ζ antibody (Figure 6, lane 5; anti-14-3-3ε antibody blot), indicating the presence of a 14-3-3ζ/ε heterodimer in the nucleus at this phase (Table 1). The β isoform, present in the G_1/S NE at approximately 3-fold higher amount, with respect to s-s (Table 1 and Figure 6, lane 4; anti-14-3-3β antibody blot), was also immunoprecipitated by anti-14-3-3ζ antibody (Figure 6, lane 5; anti-14-3-3β antibody blot), indicating that a 14-3-3ζ/β heterodimer also exists in the nucleus in this phase (Table 1). In contrast, even though the amount of both the γ and the σ isoforms in the G_1/S NE increased by approximately 28- and 4-fold, respectively, by comparison to s-s (Table 1 and Figure 6, lane 4; anti-14-3-3γ and anti-14-3-3σ antibody blots), neither isoform was immunoprecipitated by the anti-14-3-3ζ antibody, suggesting that neither 14-3-3ζ/γ nor 14-3-3ζ/σ heterodimers were present in the nucleus at G_1/S (Table 1 and Figure 6, lane 5; anti-14-3-3γ and anti-14-3-3σ antibody blots). Similarly, these two isoforms (γ and σ) were not detected at the G_2/M IP (Figure 6, lane 8; anti-14-3-3γ and anti-14-3-3σ antibody blots) despite the fact that their nuclear amount was increased by approximately 80- and 5-fold, respectively, in G_2/M (Table 1 and Figure 6, lane 7; anti-14-3-3γ and anti-14-3-3σ antibody blots). The β and ε isoforms were detected in both the G_2/M phase NE (Table 1 and Figure 6, lane 7; anti-14-3-3β and anti-14-3-3ε antibody blots), where their nuclear amount was increased by approximately 6- and 53-fold, respectively, with respect to the amount in s-s NE (Table 1), and the G_2/M IP (Figure 6, lane 8; anti-14-3-3β and anti-14-3-3ε antibody blots), indicating that both heterodimeric combinations were present in the nucleus at G_2/M (Table 1). The anti-14-3-3ζ antibody IP was controlled with an immunoprecipitation performed with NRS, and no trace of any of the 14-3-3 isoforms was detected at each phase (Figure 6, lanes 3, 6, and 9; all blots). These results are summarized in Table 1. WCE from log phase cells were used as positive control for the immunodetection with all the anti-14-3-3 antibodies (Figure 6, left-extreme lane).

r14-3-3ζ-MBP Increases in Vitro DNA Replication Activity of HeLa Extracts. The anti-14-3-3 antibodies against isoforms β, γ, ε, ζ, and σ were previously found to decrease in vitro DNA replication because of interference with the formation of the CBP−cruciform DNA complex (*18*, *19*), while an anti-cruciform DNA antibody was able to increase the basal level of in vitro DNA replication (*4*). Here, we analyzed the effect of r14-3-3ζ-MBP on the in vitro DNA replication of p186, using a mammalian in vitro replication system (*36*). The effect of preincubating increasing amounts (0.75, 1.5, and 7.5 μg) of r14-3-3ζ-MBP with HeLa cell WCE was analyzed (Figure 7). The products of p186 replication (not shown) were quantified after digestion by DpnI, a restriction endonuclease that digests fully methylated DNA at the sequence GmATC, as previously described (*18*, *19*). Template p186 DNA, which is propagated in dam^+ bacteria, is fully methylated and digested, while newly replicated p186 DNA in dam^- mammalian cell extracts is resistant to digestion by DpnI. Preincubation of HeLa extracts with increasing amounts of r14-3-3ζ-MBP progressively increased the level of DNA replication, by comparison to the control reaction, lacking addition of r14-3-3ζ-MBP (Figures 7). While preincubation with 0.75 μg of the recombinant protein (approximately 0.5% of the total protein) had a modest effect on p186 replication (Figure 7, bar 2), the replication level being comparable to the control reaction (1 relative unit), in which HeLa cell extracts were preincubated with elution

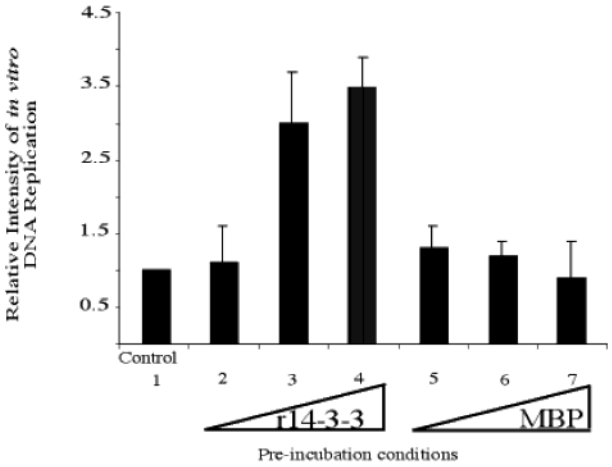

FIGURE 7: r14-3-3ζ-MBP increases in vitro DNA replication. 150 μg of HeLa WCE (see Experimental Procedures) was preincubated with either elution buffer (control; bar 1) or 0.75 μg (bar 2), 1.5 μg (bar 3), and 7.5 μg (bar 4) of r14-3-3ζ-MBP or with respective equimolar amounts of MBP (bars 5−7). The bars represent the quantification of the p186 DNA bands that were resistant to digestion by DpnI (1.5 U, 1 h, 37 °C) after an in vitro replication reaction.

buffer (Figure 7, bar 1), preincubation with 1.5 μg (approximately 1% of the total protein) increased in vitro DNA replication by 3-fold (Figure 7, bar 3). By further increasing the amount of r14-3-3ζ-MBP in the extracts 5-fold (approximately to 5% of the total protein), the replication activity was only slightly further increased (Figure 7, bar 4). The level of in vitro replication activity was not changed when increasing equimolar amounts (0.43, 0.86, and 4.3 μg) of MBP alone were preincubated with the HeLa extracts (Figure 7, bars 5−7).

DISCUSSION

Cruciform structures, extruded from IR sequences, have been involved in the initiation of DNA replication (*1*−*5*), and a cruciform binding protein, CBP, has been previously purified from HeLa cells (*14*). On the basis of microsequence analysis of tryptic peptides, it was shown that CBP belongs to the 14-3-3 family of proteins (*16*). Here, we have produced a fusion protein r14-3-3ζ-MBP and analyzed its ability to bind to cruciform DNA, the conditions under which this binding was possible, and the effect of this recombinant protein on mammalian in vitro DNA replication.

The 14-3-3ζ cDNA was cloned in the plasmid pmal-c2X using the Xba1 and EcoR1 restriction sites, having an MBP tag at the 5′ end. Bacterial expression and purification of the recombinant 14-3-3ζ-MBP yielded a highly pure fusion protein (data not shown). The pure r14-3-3ζ-MBP had no cruciform−DNA binding activity (Figure 1), in contrast to the CBP-enriched fraction (F_{TH}, ref *16*). Using a similar cloning and expression strategy, Jones et al. (*31*) previously expressed in bacteria the 14-3-3 isoforms ϵ and τ, which were both shown to be active, the ϵ isoform by phosphorylation, using the protein kinase C (PKC) assay, and the τ isoform by inhibition of PKC assay (*31*). Thus, it was unlikely that r14-3-3ζ-MBP did not show cruciform binding activity because the polypeptide was not properly folded in bacteria. One possible reason might be that the MBP tag (N-terminal located) was either interfering with the binding to cruciform DNA or preventing the protein from dimerizing, a requirement for attaining cruciform binding activity (*14*−*16*, *18*, *19*). For this, the dimerization state of r14-3-3ζ-MBP was analyzed by BN−PAGE followed by Coomasie staining before and after digestion by Factor XA (Figure 2A), an enzyme that cleaves the fusion protein at a translated polylinker region between the r14-3-3ζ and the MBP tag (New England Biolabs). It was observed that the fusion protein was not completely digested by Factor XA, confirming a previous report and suggesting that the 14-3-3 portion had the correct conformation (*31*) since both undigested (r14-3-3ζ-MBP/r14-3-3ζ-MBP) and partially digested (r14-3-3ζ-MBP/r14-3-3ζ) products were detected as specific bands of approximately 140 and 100 kDa, respectively. This result indicated that the MBP tag did not interfere with dimerization of r14-3-3ζ. The Factor XA digestion products, which contained r14-3-3ζ dimers (r14-3-3ζ/r14-3-3ζ), had no cruciform DNA binding activity either, while F_{TH} collected from the amylose column had, indicating that the lack of CBP activity of r14-3-3ζ-MBP was not due to its denaturation by passage through the amylose column (Figure 2B). Pure r14-3-3ζ-MBP, however, was able to bind to cruciform DNA after having been preincubated with F_{TH} (Figure 3). In a previous study (*21*), it was found that the *S. cerevisiae* 14-3-3 homologues, Bmh1p and Bmh2p, were only able to bind cruciform DNA when both isoforms were present in the *S. cerevisiae* nuclear extracts and not when either isoform was present alone. These two independent findings suggested that heterodimerization or a specific combination of 14-3-3 isoforms might be essential for cruciform DNA binding. The 14-3-3 dimer central groove, the proposed cruciform DNA binding region (*15*), has a specific shape and size that allows cruciform DNA binding. CBP/14-3-3 binding to cruciform DNA had previously been shown to be specific for the cruciform structure and not its nucleotide sequence (*14*, *16*). It has not been shown, however, whether CBP requires a specific alignment of its amino acids or whether the 3-D orientation of the side chain of the amino acids involved in cruciform DNA binding is relevant for CBP activity. The number of 14-3-3 isoform combinations that form heterodimers with CBP activity may be limited. It has been proposed that residues 9−16 of the N-terminal domain, the dimerization interface region, of all 14-3-3 isoforms are highly variable, limiting the number of possible homo- or heterodimeric combinations formed (*24*, *25*). This restriction might confer specificity to 14-3-3 functions, including cruciform DNA binding. The presence of r14-3-3ζ-MBP in the isolated CBP−cruciform DNA complex further confirmed that the MBP tag fused to 14-3-3ζ did not prevent binding of r14-3-3ζ-MBP to cruciform DNA and suggested that r14-3-3ζ-MBP was able to dimerize with certain endogenous 14-3-3 isoforms and attain cruciform binding activity. On the other hand, it has been reported that dimers of 14-3-3 are stable and do not readily exchange (*25*, *28*). The data presented here, however, are not in conflict with those reports since it was found that at least a 3-h preincubation time was required to observe both heterodimerization (Figure 3E) and CBP activity (Figure 3F) in a r14-3-3ζ-MBP/F_{TH} mixture, and even after an 18-h incubation, only approximately a quarter of the input r14-3-3ζ-MBP had been heterodimerized (Figure 3E) or attained cruciform binding activity (Figure 3F). The observed CBP activity of r14-3-

3ζ-MBP was not due to the presence of the F_{TH} buffer components since r14-3-3ζ-MBP eluted with F_{TH} buffer did not react with cruciform DNA either (Figure 1). The fact that no endogenous 14-3-3 was detected in r14-3-3ζ-MBP fractions eluted after the passage of F_{TH} through an amylose column, where r14-3-3ζ-MBP was bound (Figure 3D), indicated that endogenous 14-3-3 isoforms present in the F_{TH} did not simply stick to r14-3-3ζ-MBP, but rather, they heterodimerized with it.

In support of this conclusion, we found that the recombinant protein co-immunoprecipitated with three endogenous 14-3-3 isoforms—β, ϵ, and ζ—after having been preincubated with F_{TH} (Figure 4B−D), while other isoforms, such as γ and σ, did not interact with it. This result suggested that r14-3-3ζ-MBP needs to heterodimerize with the endogenous β and/or the ϵ isoform to have cruciform binding activity. Dimerization of r14-3-3ζ-MBP with the endogenous ζ isoform would be similar to a homodimerization of two 14-3-3ζ polypeptides, and these dimers did not have cruciform binding activity (Figure 2B). Jones et al. (*28*) had previously demonstrated, by a similar method, that recombinant 14-3-3ϵ dimerized with endogenous 14-3-3ϵ and heterodimerized with endogenous 14-3-3ζ. The β and ζ isoforms have not been shown before to form a heterodimer, but both are the only 14-3-3 isoforms found to interact with Raf-1 kinase (*31*, *40*−*42*), suggesting that in their role as chaperone proteins they may interact to bring two Raf molecules together, supporting Raf/Raf dimer formation. In fact, it has been suggested that 14-3-3 reactivates Raf by promoting the formation of Raf dimers (*43*). The ability of r14-3-3ζ-MBP to heterodimerize with the β and ϵ 14-3-3 isoforms was further tested with NE from HeLa cells that had been either serum-starved (s-s) or blocked at the G_1/S or G_2/M phases of the cell cycle. WCE and NE were prepared from these cells and immunoblotted against 14-3-3 isoforms β, γ, ϵ, ζ, and σ (Figure 5B) to monitor the expression and nuclear presence of these isoforms throughout the cell cycle. The NE contained some cytoplasmic contamination that did not significantly alter the interpretation of the data since Cas/p130 (Crk-associated substrate) and Crk proteins, both exclusively cytoplasmic (*39*), were present in less than 0.5% in NE from the s-s, G_1/S, and G_2/M HeLa cells (Figure 5A). Cas/p130 has been reported to function as an adapter protein for CrkII to elicit cell migration responses (*39*) and interacts with cytoplasmic 14-3-3 proteins upon cell adhesion (*44*). The presence of Ku70, an abundant multifunctional nuclear protein that is also involved in DNA replication (*38*), was tested as positive control for the Western blot analyses of WCE and NE. Immunoblotting of the WCE and NE with anti-14-3-3β, γ, ϵ, σ, and ζ antibodies revealed that the total expression of all these isoforms was higher at the G_1/S and G_2/M phases of the cell cycle, particularly the expression of the σ and γ isoforms (Figure 5B). In addition to their role in cell signaling pathways, which would require the cytoplasmic presence of these proteins at all phases of the cell cycle, their role as check-point proteins (*18*, *19*, *45*−*51*) may explain this increased expression. On the other hand, expression of the human replication origin binding protein, hOrc2p, whose expression and chromatin-bound state have been shown to be stable throughout the cell cycle (*35*), was approximately the same in both the WCE and the NE at all phases of the cell cycle (Figure 5B). Interestingly, the amount of the 14-3-3 isoforms in the nuclear compartment was dramatically increased at G_1/S and G_2/M cells, particularly that of the γ and ϵ isoforms, by comparison to s-s cells. The γ isoform, for instance, was barely detected in s-s NE, and only trace amounts of the ϵ isoform were detected at this stage (Table 1 and Figure 5B). Their role in DNA replication (*18*, *19*, *52*), as well as their interaction with the check-point proteins Cdk1 and Ccd25 (*45*−*50*) and with the cell cycle arrest protein p53 (*53*) might relate to their increased presence in the nuclear compartment at G_1/S and G_2/M. The anti-14-3-3ζ antibody immunoprecipitation from the NE prepared from s-s, G_1/S, and G_2/M cells produced similar results as its recombinant counterpart (Figure 6), confirming that endogenous 14-3-3ζ also heterodimerizes with the β and ϵ isoforms, while it does not with the γ or σ isoforms (Table 1). The increased amount of these heterodimers at the onset of the S phase would be consistent with their role as DNA replication origin-binding proteins (*18*, *19*). The same heterodimers were also found at the onset of mitosis, where the nuclear amount of the 14-3-3 isoforms was slightly higher (Figure 5B), suggesting that nuclear import of the 14-3-3 isoforms increases during S and G_2 and perhaps indicating different roles of these proteins in the two phases. The presence of 14-3-3 dimers in the nucleus at the G_2/M border might be due to their role in the transition to mitosis.

Finally, the effect of r14-3-3ζ-MBP protein on in vitro replication of p186 plasmid in HeLa cell extracts was analyzed. Addition of the recombinant polypeptide to the system specifically increased the replication activity of the extracts by approximately 2.5−4-fold, while addition of MBP alone had no effect (Figure 7). Two previous pieces of evidence suggested that stabilization of cruciform structures at or near origins of DNA replication is involved in the regulation of initiation of DNA replication: (1) anti-cruciform DNA antibodies, when introduced into permeabilized cells, increased DNA replication by 2−11-fold (*4*) and (2) anti-14-3-3 antibodies specific for the β, γ, ϵ, ζ, and σ isoforms, which interfered with the formation of the CBP−cruciform DNA complex, inhibited the in vitro DNA replication activity of the HeLa extract (*18*, *19*). The data presented in this study suggest that upregulation of at least one of the 14-3-3 isoforms involved in DNA replication could eventually lead to an increase in DNA replication activity in the cell. In particular, the exogenous addition of the ζ isoform to the in vitro replication system might increase the chances of forming more active CBP molecules with its β and ϵ partners. These data support the hypothesis that cruciform stabilization at replication origins may facilitate origin recognition by proteins of the replication machinery (*4*).

Overall, the data presented in this study suggest that 14-3-3ζ, in homodimeric combination, does not have cruciform binding activity and that this activity can be attained upon heterodimerization with specific isoforms, such as β and ϵ. In addition, the enhancing effect of r14-3-3ζ-MBP on in vitro DNA replication suggests that upregulation of specific 14-3-3 isoforms might lead to increased DNA replication activity.

ACKNOWLEDGMENT

We thank Dr. Bruce Stillman (Cold Spring Harbor Laboratory, NY) for the anti-hOrc2p antibody and Dr.

Alastair Aitken (University of Edinburgh, Scotland) for the 14-3-3ζ cDNA. We also thank the undergraduate students Anne Letessier and Brian Daqing Li for technical help.

REFERENCES

1. Hand, R. (1978) *Cell 15*, 317−325.
2. Zannis-Hadjopoulos, M., Kaufmann, G., and Martin, R. G. (1984) *J. Mol. Biol. 179*, 577−586.
3. Frappier, L., Price, G. B., Martin, R. G., and Zannis-Hadjopoulos, M. (1987) *J. Mol. Biol. 193*, 751−758.
4. Zannis-Hadjopoulos, M., Frappier, L., Khoury, M., and Price, G. B. (1988) *EMBO J. 7*, 1837−1844.
5. Landry, S., and Zannis-Hadjopoulos, M. (1991) *Biochim. Biophys. Acta 1088*, 234−244.
6. Sinden, R. R., Zheng, G. X., Brankamp, R. G., and Allen, K. N. (1991) *Genetics 129*, 991−1005.
7. Palecek, E. (1991) *Crit. Rev. Biochem. Mol. Biol. 26*, 151−226.
8. Yagil, G. (1991) *Crit. Rev. Biochem. Mol. Biol. 26*, 475−559.
9. Sinden, R. R., Broyles, S. S., and Pettijohn, D. E. (1983) *Proc. Natl. Acad. Sci. U.S.A. 80*, 1797−1801.
10. Noirot, P., Bargonetti, J., and Novick, R. P. (1990) *Proc. Natl. Acad. Sci. U.S.A. 87*, 8560−8564.
11. Pearson, C. E., Zorbas, H., Price, G. B., and Zannis-Hadjopoulos, M. (1996) *J. Cell. Biochem. 63*, 9−22.
12. Ward, G. K., McKenzie, R., Zannis-Hadjopoulos, M., and Price, G. B. (1990) *Exp. Cell. Res. 188*, 235−246.
13. Ward, G. K., Shihab-El-Deen, A., Zannis-Hadjopoulos, M., and Price, G. B. (1991) *Exp. Cell. Res. 195*, 92−98.
14. Pearson, C. E., Ruiz, M. T., Price, G. B., and Zannis-Hadjopoulos, M. (1994) *Biochemistry 33*, 14185−14196.
15. Pearson, C. E., Zannis-Hadjopoulos, M., Price, G. B., and Zorbas, H. (1995) *EMBO J. 14*, 1571−1580.
16. Todd, A., Cossons, N., Aitken, A., Price, G. B., and Zannis-Hadjopoulos, M. (1998) *Biochemistry 40*, 14317−14325.
17. Xiao, B., Smerdon, S. J., Jones, D. H., Dodson, G. G., Soneji, Y., Aitken, A., and Gamblin, S. J. (1995) *Nature 376*, 188−191.
18. Novac, O., Alvarez, D., Pearson, C. E., Price, G. B., and Zannis-Hadjopoulos, M. (2002) *J. Biol. Chem. 277*, 11174−11183.
19. Alvarez, D., Novac, O., Callejo, M., Price, G. B., and Zannis-Hadjopoulos, M. (2002) *J. Cell. Biochem. 87*, 194−207.
20. Zannis-Hadjopoulos, M., Novac, O., Alvarez, D., and Price, G. B. (2002*) Biochem. Soc. Trans. 30*, 397−401.
21. Callejo, M., Alvarez, D., Price, G. B., and Zannis-Hadjopoulos, M. (2002) *J. Biol. Chem. 277*, 38416−38423.
22. Martin, H., Rostas, J., Patel, Y., and Aitken, A. (1994) *J. Neurochem. 63*, 2259−2265.
23. Brunet, A., Kanai, F., Stehn, J., Xu, J., Sarbassova, D., Frangioni, J. V., Dalal, S. N., DeCaprio, J. A., Greenberg, M. E., and Yaffe, M. B. (2002) *J. Cell Biol. 156*, 817−828.
24. Aitken, A. (1996) *Trends Cell. Biol. 6*, 341−347.
25. Aitken, A., Baxter, H., Dubois, T., Clokie, S., Mackie, S., Mitchell, K., Peden, A., and Zemlickova, E. (2002) *Biochem. Soc. Trans. 30*, 351−360.
26. Liu, Y. C., Elly, C., Yoshida, H., Bonnefoy-Berard, N., Altman, A. (1996) *J. Biol. Chem. 271*, 14591−14595.
27. Fu, H. A., Subramanian, R. R., and Masters, S. C. (2000) *Annu. Rev. Pharmacol. Toxicol. 40*, 617−647.
28. Jones, D. H., Lye, S., and Aitken, A. (1995) *FEBS Lett. 368*, 55−58.
29. Woo, K., Lou, G., Sheen, P., and Ferl, R. J. (1997) *Arch. Biochem. Biophys. 339*, 2−8.
30. Liu, D., Bienkowska, J., Petosa, C., Collier, R. J., Fu, H., and Liddington, R. (1995) *Nature 376*, 191−194.
31. Jones, D. H., Martin, H., Madrazo, J., Robinson, K. A., Nielsen, P., Roseboom, P. H., Patel, Y., Howell, S. A., and Aitken, A. (1995) *J. Mol. Biol. 245*, 375−384.
32. Abarca, D., Madueno, F., Martinez-Zapater, J. M., and Salinas, J. (1999) *FEBS Lett. 462*, 377−382.
33. Elborough, K. M., and West, S. C. (1988) *Nucleic Acids Res. 16*, 3603−3616.
34. Mah, D. C. W., Dijkwel, P. A., Todd, A., Klein, V., Price, G. B., and Zannis-Hadjopoulos, M. (1993) *J. Cell Sci. 105*, 807−818.
35. Mendez, J., and Stillman, B. (2000) *Mol. Cell. Biol. 20*, 8602−8612.
36. Pearson, C. E., Frappier, L., and Zannis-Hadjopoulos, M. (1991) *Biochim. Biophys. Acta 1090*, 156−166.
37. Todd, A., Landry, S., Pearson, C. E., Khoury, V., and Zannis-Hadjopoulos, M. (1995) *J. Cell. Biochem. 57*, 280−289.
38. Matheos, D., Ruiz, M., Price, G. B., and Zannis-Hadjopoulos, M. (2002) *Biochim. Biophys. Acta 1578*, 59−72.
39. Klemke, R. L., Leng, J., Molander, R., Brooks, P. C., Vuori, K., and Cheresh, D. A. (1998) *J. Cell Biol. 140*, 961−972.
40. Fantl, W. J., Muslin, A. J., Kikuchi, A., Martin, J. A., McNicol, A. M., Gross, R. W., and William, L. T. (1994) *Nature 371*, 612−614.
41. Fu, H., Xia, K., and Pallas, D. C. (1994) *Science 266*, 126−129.
42. Li, S., Janosch, P., Tanji, M., Rosenfeld, G. C., Waymire, J. C., Mischak, H., Kolch, W., and Sedivy, J. M. (1995) *EMBO J. 14*, 685−696.
43. Tzivion, G., Luo, Z., and Avruch, J. (1998) *Nature 394*, 88−92.
44. Garcia-Guzman, M., Dolfi, F., Rusello, M., and Vuori, K. (1999) *J. Biol. Chem. 274*, 5762−5768.
45. Su, T. T., Parry, D. H., Donahoe, B., Chien, C. T., O'Farrell, P. H., and Purdy, A. (2001) *J. Cell Sci. 114*, 3445−3454.
46. Forrest, A., and Gabrielli, B. (2001) *Oncogene 20*, 4393−4401.
47. Taylor, W. R., and Stark, G. R. (2001) *Oncogene 20*, 1803−1815.
48. Bulavin, D. V., Higashimoto, Y., Popoff, I. J., Gaarde, W. A., Basrur, V., Potapova, O., Appella, E., Fornace, A. J., Jr. (2001) *Nature 411*, 102−107.
49. Graves, P. R., Lovly, C. M., Uy, G. L., and Piwnica-Worms, H. (2001) *Oncogene 20*, 1839−1851.
50. Mils, V., Baldin, V., Goubin, F., Pinta, I., Papin, C., Waye, M., Eychene, A., and Ducommun, B. (2000) *Oncogene 19*, 1257−1265.
51. Vercoutter-Edouart, A. S., Lemoine, J., Le Bourhis, X., Louis, H., Boilly, B., Nurcombe, V., Revillion, F., Peyrat, J. P., and Hondermarck, H. (2001) *Cancer Res. 61*, 76−80.
52. Kurz, E, U., Leader, K. B., Kroll, D. J., Clark, M., and Gieseler, F. (2000) *J. Biol. Chem. 275*, 13948−13954.
53. Waterman, M. J., Stavridi, E. S., Waterman, J. L., and Halazonetis, T. D. (1998) *Nat. Genet. 19*, 175−178.

BI027343P